Synthesis and characterization of zinc oxide nanoparticles for dye-sensitized solar cells

Renata Marczak, Wolfgang Peukert
Institute of Particle Technology, Friedrich-Alexander-University Erlangen-Nuremberg, Cauerstr. 4, 91058 Erlangen, Germany

Fabian Werner, Dirk M. Guldi
Department of Chemistry and Pharmacy, Friedrich-Alexander-University Erlangen-Nuremberg, Egerlandstr. 3, 91058 Erlangen, Germany

Jan-Frederik Gnichwitz, Andreas Hirsch
Institute of Organic Chemistry, Friedrich-Alexander-University Erlangen-Nuremberg, Henkestr. 42, 91054 Erlangen, Germany

Abstract

Stable ZnO nanoparticles suitable for further derivatization of their surface were synthesized in the liquid phase from homogeneous ethanolic solutions of the precursors, lithium hydroxide and zinc acetate. The particle growth was monitored by in situ absorption spectroscopy and dynamic light scattering (DLS). It was found that the growth of the particles was governed by temperature as well as the presence of the reaction by-product lithium acetate during the ripening process. In particular, the reaction could be almost completely arrested by removal of this by-product. The "washing" consisted of repeated precipitation of the ZnO particles by addition of alkanes such as heptane, removal of the supernatant, and redispersion in ethanol. The ZnO nanoparticles, before and after "washing", were characterized by absorption spectroscopy, DLS, thermogravimetric analysis (TGA), X-ray powder diffraction (XRD) and high resolution transmission electron microscopy (HRTEM).

The functionalization of the ZnO nanoparticles with photoactive organic compounds, i.e., 5-(N-(3,4-dihydroxyphenethyl)-2-phenoxyacetamide)- 10, 15, 20-(p-tert-butyl-triphenyl)-porphyrinato-zinc and 5-(3,4-dihydroxy-N-phenylbenzamide)-10,15,20-tris(4-tert-butylphenyl) porphyrinato-zinc, was examined. Mesoporous films of the ZnO nanoparticles suitable for use as electrodes in dye-sensitized solar cells (DSSCs) were prepared by the doctor blade technique. Following sintering the films were sensitized by the dye molecules mentioned above. The morphology of the films was characterized by using scanning electron microscopy (SEM). The current generated during photoelectrochemical measurements of these films was ascribed to an efficient photoinduced electron transfer from the photoexcited porphyrin to the ZnO moiety.

Introduction

Dye-sensitized solar cells (DSSCs),[1] based on photoelectrochemical dye-sensitized mesoporous metal-oxide electrodes, have been a subject of intense interest for several years. This is due to the fact that they offer a potentially low cost, medium performance alternative to traditional photovoltaic devices.[2] In most work on DSSCs, titanium dioxide (TiO_2) has been the material of choice and so far has been shown to enable the highest overall light conversion efficiency.[1, 3] However, due to it having a similar size band gap energy, ZnO (~ 3.4 eV) has recently been explored as an alternative material for DSSCs.[4, 5] Although its potential has yet to be fully realized ZnO has significant advantages as a mesoporous electrode for DSSCs when compared to TiO_2, including much lower UV

photocatalytic activity,[5] fewer electron-trapping surface states,[5] simpler tailoring of the nanostructure and easier dye-functionalization of the surface.[6] These advantages are thought to provide a promising means for improving the overall solar cell performance by improving the working electrode in dye-sensitized solar cells.

To obtain ZnO nanostructures different synthesis routes have been devised, including solid-vapor phase thermal sublimation,[7] spray pyrolysis,[8] RF plasma synthesis,[9] sonochemical or microwave-assisted synthesis[10] and hydrothermal processing.[11] However, wet-phase synthesis of ZnO is an area of intense interest, as it provides a low-temperature, economical way to produce various ZnO nanostructures.[12, 13] Growth from solution typically starts with nucleation and is followed by growth of the nuclei by addition of dissolved species until the metal cation concentration reaches the solubility of the oxide. Then particle ageing proceeds in the mother liquors. Synthesis conditions such as temperature,[14] the overall concentration of the precursors,[15] water concentration,[16] ions present in solution[17], and solvent[18] have been shown to impact particle nucleation and growth. Therefore, the synthesis and investigation of ZnO nanoparticles suitable for further functionalization of their surface for DSSCs application is of great interest.

Herein, we report about a simple colloidal method to synthesize ZnO nanoparticles suitable for further derivitization of their surface. The particles were prepared from zinc acetate dihydrate in ethanolic solution under basic conditions. To learn more about the growth mechanism, we have employed in situ Uv-vis absorption spectroscopy and dynamic light scattering (DLS) to quantify both particle size and energy band gap as a function of time in order to study influence of the ageing conditions on the growth of the ZnO nanocrystals. Next, we describe the photosensitization of mesoporous films of the ZnO nanoparticles by dye molecules, i.e., 5-(*N*-(3,4-dihydroxyphenethyl)-2-phenoxyacetamide)-10, 15, 20-(p-tert-butyl-triphenyl)-porphyrinato-zinc and 5-(3,4-dihydroxy-N-phenylbenzamide)-10,15,20-tris(4-tert-butylphenyl) porphyrinato-zinc (Scheme 1), for use as electrodes in dye-sensitized solar cells (DSSCs).

Experimental

All chemicals (analytical grade reagents) were purchased from commercial sources and used without further purification. Colloidal ZnO nanoparticles were prepared by hydrolyzing zinc acetate dihydrate in basic ethanol solution. The overall preparation procedure was adapted from Spanhel, Anderson[12] and Meulenkamp[13] with a few modifications. Homogenous solutions containing 0.1 M Zn^{2+} and 0.14 M OH^- were prepared by dissolving separately the reactants in boiling ethanol at atmospheric pressure. Both solutions were cooled to synthesis temperature. A white powder of anhydrous zinc acetate precipitated in a range close to room temperature.[13] The lithium hydroxide solution was added dropwise to the zinc acetate solution under vigorous stirring. A molar ratio of $[Zn^{2+}]/[OH^-]$ ratio was adjusted to 0.71. The reaction mixture became transparent after addition of about 1/3 volume of the lithium hydroxide solution. The ZnO sol was stored at ≤ 10 °C to prevent rapid particle growth. Next, the ZnO sol was washed by repeated flocculation of ZnO induced by addition of n-heptane. The supernatant was removed by centrifugation and decantation. For colloidal characterization the ZnO flocculates were redispersed in ethanol. In order to obtain the powder, the ZnO white precipitate was dried under nitrogen for about 5 minutes.

In order to obtain the 5-(N-(3,4-dihydroxyphenethyl)-2-phenoxyacetamide)- 10, 15, 20-(p-tert-butyl-triphenyl)-porphyrinato-zinc (DOPAZ) a solution of 500 mg of 5-(p-tert-butyl-acetato-phenoxy)-10, 15, 20-(p-tert-butyl-triphenyl)-porphyrin[19] (0.55 mmol) and 200 mL formic acid was stirred for 4 hours to obtain the deprotected acid. The completed reaction was observed via TLC. After that period the solvent was removed on a rotary evaporator, transferred into toluene and evaporated twice. The product was finally dried under reduced

pressure. The dried product was dissolved in dichloromethane-DMF 1:1 mixture at 0° C. 315 mg of EDC (1.65 mmol), 222 mg HOBT (1.65 mmol) and 200 mg DMAP (1.65 mmol) were added and the solution was stirred for one hour at 0° C. After that period 155 mg of Dopamin (0.825 mmol) were added to the solution and the mixture was stirred at room temperature for 48 hours. The solvent was removed on a rotary evaporator and the residue was purified with column chromatography on silica gel with a mixture of dichloromethane/methanol (19:1) as eluent. The product was obtained by crystallization in pentane. The yield was 250 mg (45%).110 mg of 5-(N-(3,4-dihydroxyphenethyl)-2-phenoxyacetamide)- 10, 15, 20-(p-tert-butyl-triphenyl)-porphyrin (0.11 mmol) was dissolved in THF and 80 mg of zinc acetate (0.44 mmol) was added. The mixture was heated to reflux over a period of 4 hours. The reaction was monitored by TLC by the disappearance of the free porphyrin. The solvent was removed on a rotary evaporator and the residue was dissolved again in dichloromethane and filtered to remove any unreacted zinc acetate. The dried product was purified with column chromatography on silica gel with a mixture of dichloromethane/methanol (95:5) as eluent. Final crystallization in pentane gave a purple red solid in good yields (40 mg, 35%). To synthesise 5-(3,4-dihydroxy-N-phenylbenzamide)-10,15,20-tris(4-tert-butylphenyl) porphyrinato-zinc (CAMIZ) 100 mg of 3,4-diphenylmethylenedioxyprotocatechuic acid[20] (0.31mmol) was dissolved in 200 mL dichloromethane at 0° C then 130 mg of DCC (0.62 mmol) and 85 mg HOBT (0.62 mmol) were added and the solution was stirred for one hour at 0° C. After that period 250 mg of 5-(4-aminophenyl)-10,15,20-tris(4-tert-butylphenyl)porphyrin[21] (0.62 mmol) were added to the solution and the mixture was stirred at room temperature for 96 hours. The solvent was removed on a rotary evaporator and the residue was purified by column chromatography on silica gel with dichloromethaneas eluent. The yield was 120 mg (35%). 100 mg of the dried residue were dissolved in 100 mL of formic acid. The solution was stirred further for 5 hours. The progress of the reaction can be monitored via TLC. After completion of the reaction, the solvent was removed by rotary evaporation. The mixture was transferred into toluene and evaporated twice. The final product is obtained by recrystallization in toluene over night at 0°C with a yield of 83 mg (98%). 80 mg of 5-(3,4-dihydroxy-N-phenylbenzamide)-10,15,20-tris(4-tert-butylphenyl) porphyrin (0.09 mmol) was dissolved in 50 mL THF and 65 mg of zinc acetate (0.36 mmol) was added. The mixture was heated to reflux over a period of 4 hours. The reaction was monitored by TLC by the disappearance of the free porphyrin. After completion of the reaction water is added till the product is precipitated. The solid is filtered and then dried in vacuum to give the desired product in a nearly quantitative yield (81 mg, 95%).

Particle size distribution, zeta potential and conductivity of ZnO nanoparticle suspensions were determined via dynamic light scattering (DLS) by using a Malvern Nano ZS Instrument with a 633 nm “red” laser. For each sample ten measurements were performed and the average value per sample was calculated. The optical properties of the nanoparticles were determined from Uv-vis absorption spectra recorded with a Cary 100 Scan Spectrometer (Varian). Spectra from colloidal suspensions were obtained with 10 mm cells. Structural analysis of the ZnO nanoparticles was performed in a D8 Advance (Bruker AXS) X-Ray diffractometer (XRD) using Cu-Kα radiation (0.154 nm). The measurement was in the range of $20° \leq 2\theta \leq 70°$. Ultra thin carbon films on a 200 mesh Cu-grid were used to place the samples for high resolution transmission electron microscopy (HRTEM) observations. The HRTEM images were obtained using a Philips CM 300 UltraTwin microscope. The measurements were carried out at an acceleration voltage of 300 kV in the dark-field mode.

Mesoporous films of the ZnO nanoparticles were prepared by the doctor blade technique.[22] For the preparation of the starting coating paste, 0.10 g of starch was solubilised in 0.75 g of ethanol and then 0.15 g of the ZnO nanoparticles were added to the

solution. Pieces of F:SnO_2 conducting glass (8Ω/cm^2 TCO) were cleaned subsequently with water, acetone and isopropanol in an ultrasonic bath. A drop of the ZnO paste was then applied to a piece of F:SnO_2 conducting glass on one of the bare edges of the substrate and flattened with a glass rod by sliding over the tape-covered edges. Such prepared films were dried at 80°C for 10 min and heated at 30°C min^{-1} to 450 °C; this temperature was held for 30 min. Next, the films were cooled slowly down to room temperature. The morphology of the films was examined by scaning electron microscope (SEM). The images were obtained by using a Zeiss Gemini Ultra 55 SEM. The measurements were carried out at the acceleration voltage of 20 kV in the dark-field mode.

Photoelectrochemical measurements were carried out in a custom made cell holder with the dye molecule/mesoporous ZnO/F:SnO_2 working electrode and a Platinum coated F:SnO_2 counter electrode. The electrolyte was 0.6 M 1,2-dimethyl-3-propylimidazolium iodide, 0.1 M lithium iodide and 0.05 M iodine in methoxyacetonitrile. Photocurrent measurements were carried out using a Keithley Sourcemeter 2400 during illumination. A collimated light beam from a adjustable 1000 W Xenon arc lamp was used for UV and VIS illumination closely matching AM 1.5 conditions. When white light was used, a 350 nm cut-off filter was used. When recording the photoaction spectrum, a B&M Spektronik grating monochromator was introduced into the path of the excitation beam for selecting the required wavelengths. All measurements were performed after subtracting stable dark current. The incident photon-to-current conversion efficiency (IPCE) defined as the number of electrons collected per incident photon, was determined from short-circuit photocurrent measurements at different wavelengths. All experiments were performed at room temperature.

Results and discussion

ZnO nanoparticles were prepared from zinc acetate dihydrate in ethanolic solution under basic conditions. The zinc acetate and lithium hydroxide solutions in ethanol were mixed at different temperatures under vigorous stirring. In order to follow the progress of the oxide formation, the suspensions of the nanoparticles were aged in their mother liquors. The influence of nanocrystal size on the electronic structure of semiconducting material is represented by the band gap increasing with decreasing of the particle size, which is attributed to the so-called quantum confinement effect. ZnO shows this effect for particles smaller than 8 nm.[23] Hence, Uv-vis absorption spectra provide a convenient way to investigate particle growth. Figure 1 shows the absorption spectra of the ZnO suspension recorded immediately after the preparation (about 2 minutes) and performed in 20 minutes intervals for about 14 h. Just after mixing the zinc acetate with the lithium hydroxide the absorbance spectrum shows a well-defined exciton peak, which suggests a very fast nucleation. Beside, a meaningful red shift in the absorption onset was observed during the early formation stage, which is attributed to the fast crystal growth. Additionally, the absorption measurements provide a qualitative indication of the crystal size distribution. The sharp excitonic peak in the absorption spectra in the case of small nanocrystals (at shorter times) is indeed indicative of the narrow size distribution of the nanoparticles in the sample. For the larger particles, sharp excitionic features are not present in the absorption spectra (at longer times), but only a broad and featureless absorption edge. This is due to the fact that a number of exciton peaks appear at different energies corresponding to different sized nanocrystals which overlap with each other. Therefore, a broadened size distribution of the nanocrystals can be expected. This assumption is confirmed by the number size distributions recorded by using DLS at different times during the aging of the particles (Figure 2). The longer the aging time, the larger particles with broader size distributions were obtained. The influence of the ageing temperature, i.e. 2 °C, 15 °C, 25 °C and 35 °C, on the particle growth was examined. The higher the temperature the larger

ZnO nanocrystals were formed, which is confirmed by the hydrodynamic diameter changes during the ZnO nanoparticle ageing recorded by DLS (Figure 3). These results show that the nanocrystals continued to age after the synthesis, even when stored at low temperatures. The ability to obtain various particle sizes is based on the phenomena that the growth of the particles is governed by temperature and time, but also by the presence of the reaction byproduct lithium acetate during the ageing process. The reaction could be almost completely stopped by removing the byproduct. This process, so-called "washing", consisted of reversible flocculation of the ZnO nanoparticles by addition of n-heptane after about four hours of ageing.[13] The particles precipitated immediately after adding heptane to the ethanolic suspension. After centrifugation and removing of the supernatant, the white ZnO flocculates were either redispersed in ethanol by using ultrasonic bath to obtain a transparent suspension or dried under nitrogen for about 5 minutes to get a white powder.

Structural analysis of the sample was performed by using X-Ray diffraction. In the XRD pattern of the ZnO nanoparticles (Figure 4) no impurity peaks are observed. All the diffraction peaks are well assigned to standard hexagonal phase ZnO with a wurtzite structure reported in JCPDS card (No. 36-1451, a = 3.249 Å, c = 5.206 Å). The broadness of the XRD peaks reveals the nanocrystalline nature of the ZnO powder. The average crystallite size of about 5 nm was estimated by using the Debye-Scherrer's equation.[24] The crystalline nature of the ZnO nanoparticles is evidenced also in the HRTEM image (Figure 5) by the clearly observed lattice features.

The ZnO nanoparticles were used for preparation of mesoporous films of the ZnO nanoparticles by the doctor blade technique. The surface morphology of the prepared nanostructured ZnO films was investigated by SEM. The SEM image shows that the ZnO particles form a porous film (Figure 6) suitable for DSSCs application. Next, the ZnO films were immersed into a 5 mM ethanolic solution of a dye-molecule and characterized as a photoelectrochemical cell with a Pt-counter electrode. Upon preparation of the F:SnO_2/mesoporous ZnO-dye molecule/Iodine-Iodide/Pt cell its photoaction spectra were recorded (Figure 7). An excellent match between the photoaction spectrum and the absorption spectrum of the dye molecule is observed. Both the Soret- (at 424 nm) and *Q*-band (550 and 600 nm) features are discerned. This photoaction spectrum confirms the origin of the photocurrent generation, namely, the chromophore activity of the dye molecule which is mainly responsible for the observed photocurrent. To conclude, the following electron-transfer sequence should be anticipated as a basis for the photocurrent generation: (i) initial photoexcitation of the dye molecules, (ii) charge separation between the photoexcited dye molecules and ZnO, (iii) electron shift from the reduced ZnO to the F:SnO_2 electrode, and (iv) electron transfer from the redox couple in the electrolyte to the oxidized dye molecules.

Conclusions

We have synthesized ZnO nanoparticles in ethanol by using a simple colloidal method. It was shown that the growth of the particles was governed by temperature as well as the presence of the reaction byproduct lithium acetate during the ageing process. This process could be almost completely stopped by removal of this byproduct by repeated flocculation of the ZnO particles by addition of n-heptane. We have shown the preparation of mesoporous films of the ZnO nanoparticles suitable for use as electrodes in dye-sensitized solar cells (DSSCs) and successful functionalization of the surface of the particles by dye molecules, i.e., 5-(N-(3,4-dihydroxyphenethyl)-2-phenoxyacetamide)- 10, 15, 20-(p-tert-butyl-triphenyl)-porphyrinato-zinc and 5-(tris-ethoxy-silane-propyl-amide-acetato-phenoxy)- 10, 15, 20-(p-tert-butyl-triphenyl)-porphyrinato-zinc. The current generated during photoelectrochemical measurements of these films was ascribed to an efficient photoinduced electron transfer from the photoexcited porphyrin to the ZnO moiety.

References

1. O'Regan, B.; Grätzel, M. *Nature* **1991**, *353*, 737.
2. Westermark, K.; Rensmo, H.; Siegbahn, H.; Keis, K.; Hagfeldt, A.; Ojamae, L.; Persson, P. *J. Phys. Chem. B* **2002**, *106*, 10102.
3. a) Green, M. A.; Emery, K.; King, D. L.; Hishikawa, Y.; Warta, W. *Prog. Photovol.: Res. Appl.* **2006**,*14*, 455. b) Hagfeldt, A.; Grätzel, M. *Acc. Chem. Res.* **2000**, *33*, 269. c) Grätzel, M. *J. Photochem. Photobiol. C* **2003,** *4*, 145.
4. a) Quintana, M.; Edvinsson, T.; Hagfeldt, A.; Boschloo, G. *J. Phys. Chem. C* **2007**, *111*, 1035. b) Redmond, G.; Fitzmaurice, D.; Grätzel, M. *Chem. Mater.,* **1994**, *6*, 686.
5. Zeng, L.; Dai, S.; Xu, W.; Wang, K. *Plasma Science & Technology* **2006**, *8*, 172.
6. Kakiuchi, K.; Hosono, E.; Fujihara, S. *J. Photochem. Photobiol. A* **2006**, *179*, 81.
7. Wang, Z. L. *J. Phys. Condens. Matter* **2004**, *16*, R829.
8. a) Park, S. B.; Kang, Y. C. *J. Aeroslo Sci.* **1997**, *28*, S473. b) Okuyama, K.; Lenggoro, I. W. *Chem. Eng. Sci.* **2003**, *58*, 537.
9. Sato, T.; Tanigaki, T.; Suzuki, H.; Saito, Y.; Kido, O.; Kimura, Y.; Kaito, C.; Takeda, A.; Keneko, S. *J. Cryst. Growth* **2003**, *255*, 313.
10. a) Hu, X. L.; Zhu, Y. J.; Wang, S. W. *Mater. Chem. Phys.* **2004**, *88*, 421. b) Hong, R. Y.; Shen, Z. H.; Li, H. Z. *J. Process Eng.* **2005**, *5*, 693.
11. a) Zhang, H.; Yang, D.; Ji, Y.; Ma, X. Y.; Xu, J.; Que, D. L. *J. Phys. Chem. B* **2004**, *108*, 3955., b) Liu, B.; Zeng, H. C. *J. Am. Chem. Soc.* **2003**, *125*, 4430.
12. Spanhel, L; Anderson, M. A. *J. Am. Chem. Soc.* **1991**, *113*, 2826.
13. Meulenkamp, E. A. *J. Phys. Chem. B* **1998**, *102*, 5566.
14. Wong, E. M.; Bonevich, J. E.; Searson, P. C. *J. Phys. Chem. B* **1998**, *102*, 7770.
15. a) Pacholski, C.; Kornowski, A.; Weller, H. *Angew. Chem. Int. Ed.* **2002**, *41*, 1188. b) Verges, M. A. Mifsud., A.; Serna, C. J. *J. Chem. Soc. Faraday Trans.* **1990**, *86*, 959.
16. Hu, Z.; Escamilla Ramirez, D. J.; Heredia Cervera, B. E.; Oskam, G.; Searson, P. C. *J. Phys. Chem. B* **2005**, *109*, 11209.
17. a) Hu, Z.; Oskam, G.; Penn, R. L.; Pesika, N.; Searson, P. C.; *J. Phys. Chem. B*. **2003**, *107*, 3124. b) Hu, Z.; Herrera Santos, J. F.; Oskam, G.; Searson, P. C.; *J. Colloid. Interface Sci.* **2005**, *288*, 313.
18. Hu, Z.; Oskam, G.; Searson, P. C. *J. Colloid Interface Sci.* **2003**, *263*, 454.
19. Wessendorf, F.; Gnichwitz, J.-F.; Sarova, G. H.; Hager, K.; Hartnagel, U.; Guldi, D. M.; Hirsch, A. *J. Am. Chem. Soc*. **2007**, *129*, 16057.
20. Iacazio, G.; Perissol, C.; Faure, B. *Journal of Microbiological Methods* **2000**, *42*, 209.
21. Liu, X.; Liu, J.; Jin, K.; Yang, X.; Peng, Q.; Sun, L. *Tetrahedron* **2005**, *61*, 5655.
22. Ito, S. *J. Mater. Chem.* **2004**, *14*, 385.
23. a) Koch, U.; Fojtik, A.; Weller, H.; Henglein, A. *Chem. Phys. Lett.* **1985**, *122*, 507. b) Wong, E. M.; Bonevich, J. E.; Searson, P. C. *J. Phys. Chem. B* **1998**, *102*, 7770. c) Brus, L. E. *J. Phys. Chem. B* **1986**, *90*, 2555.
24. West, A. R. Solid State Chemistry and Its Applications, John Wiley & Sons: New York, 1984; pp. 174-175.

a)

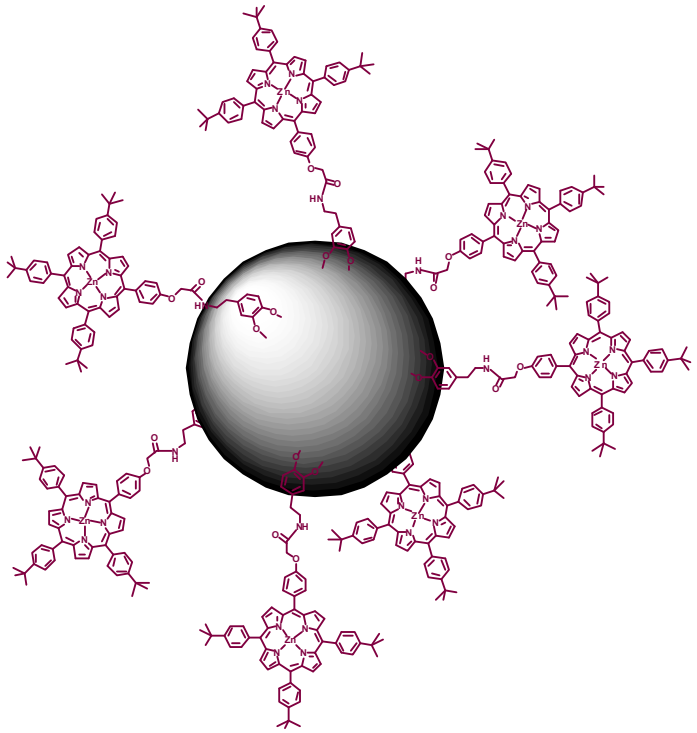

b)

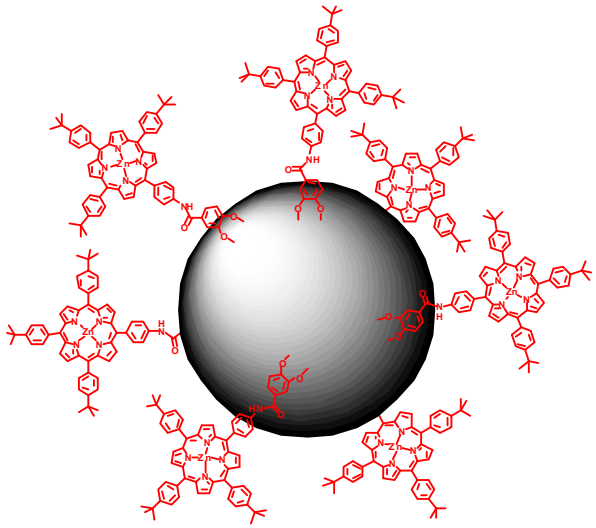

Scheme 1. a) 5-(N-(3,4-dihydroxyphenethyl)-2-phenoxyacetamide)- 10, 15, 20-(p-tert-butyl-triphenyl)-porphyrinato-zinc (DOPAZ) and b) 5-(3,4-dihydroxy-N-phenylbenzamide)-10,15,20-tris(4-tert-butylphenyl) porphyrinato-zinc (CAMIZ) molecules adsorbed on the surface of a ZnO nanoparticle.

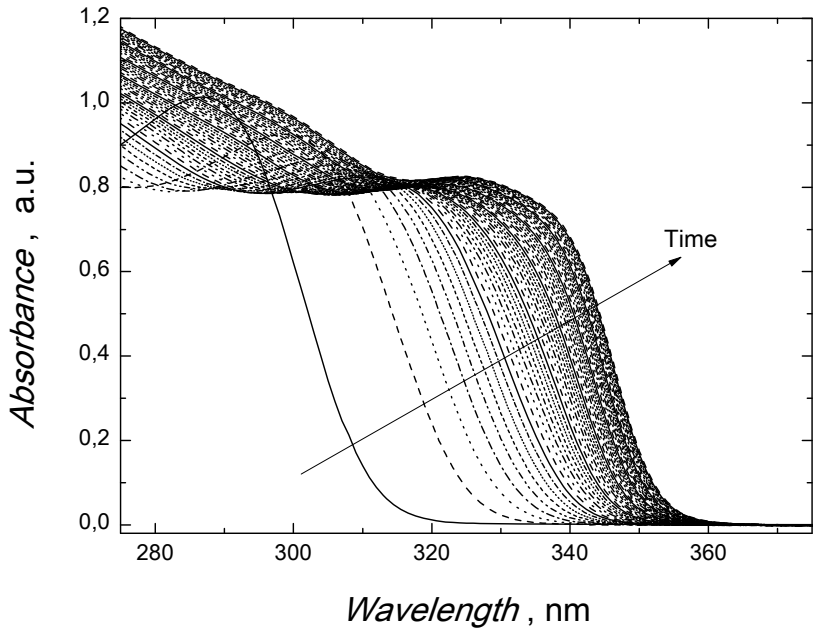

Figure 1. Room temperature absorption spectra recorded at different aging time of ZnO nanocrystals in ethanolic suspension at 35°C.

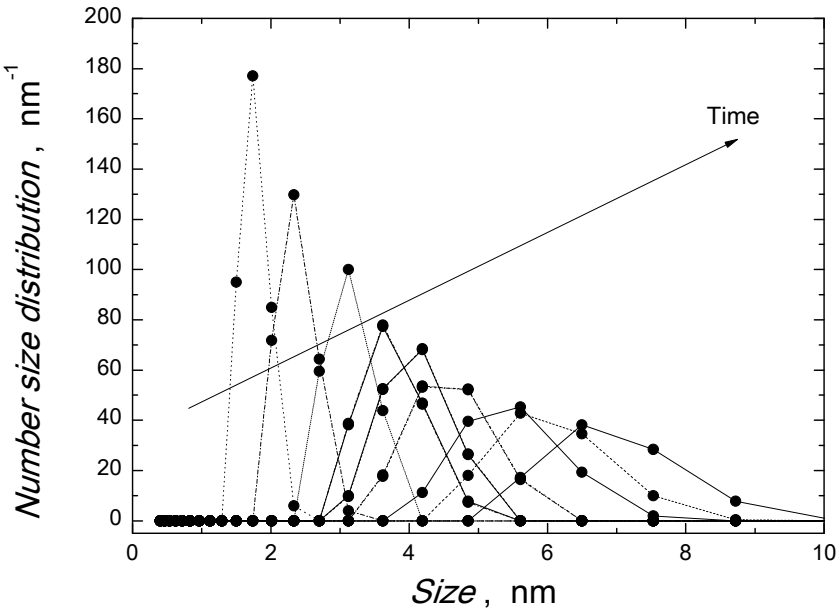

Figure 2. Number size distributions recorded by DLS at different aging time of the ZnO crystals in ethanolic suspension at 35 °C.

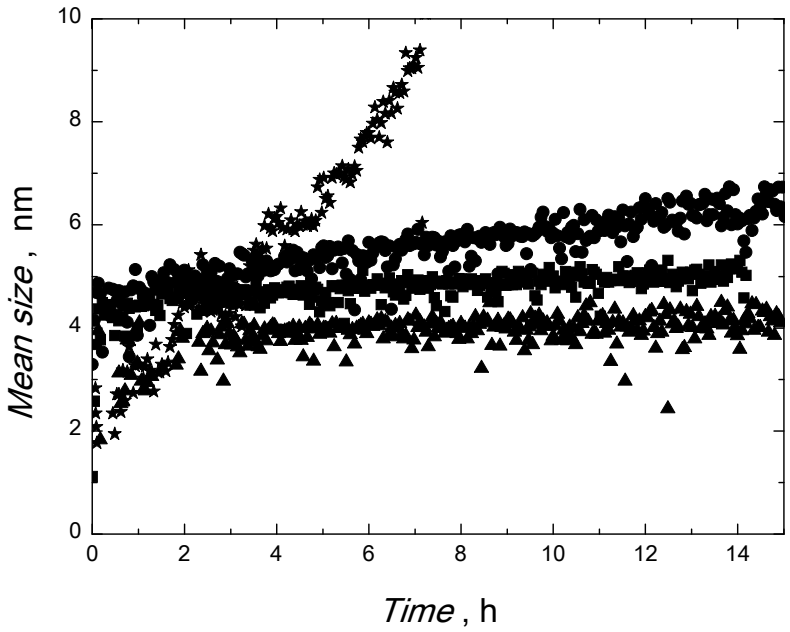

Figure 3. Particle ageing in the ZnO ethanolic suspension at 2 °C (triangles), 15 °C (squares), 25 °C (circles) and 35 °C (stars) monitored by DLS.

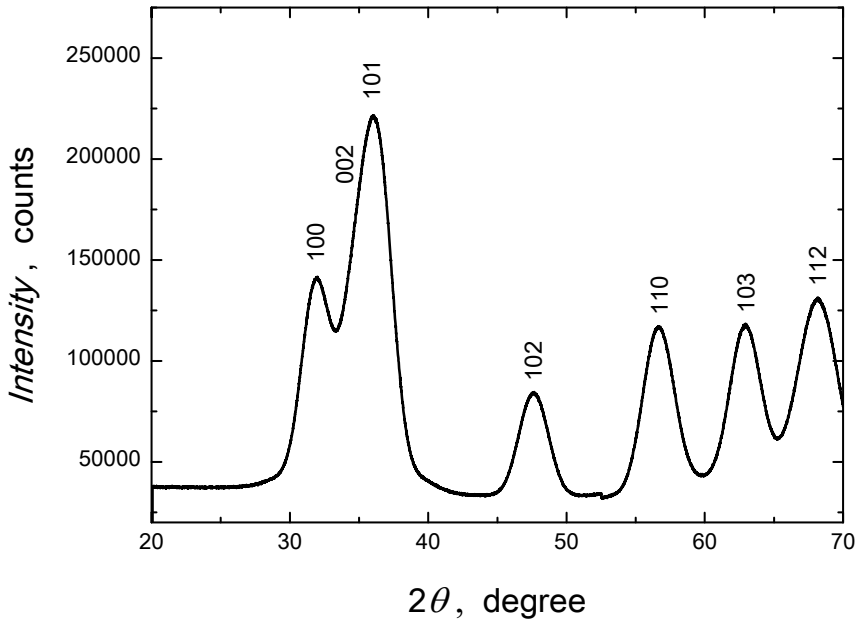

Figure 4. X-ray powder pattern of ZnO nanoparticles.

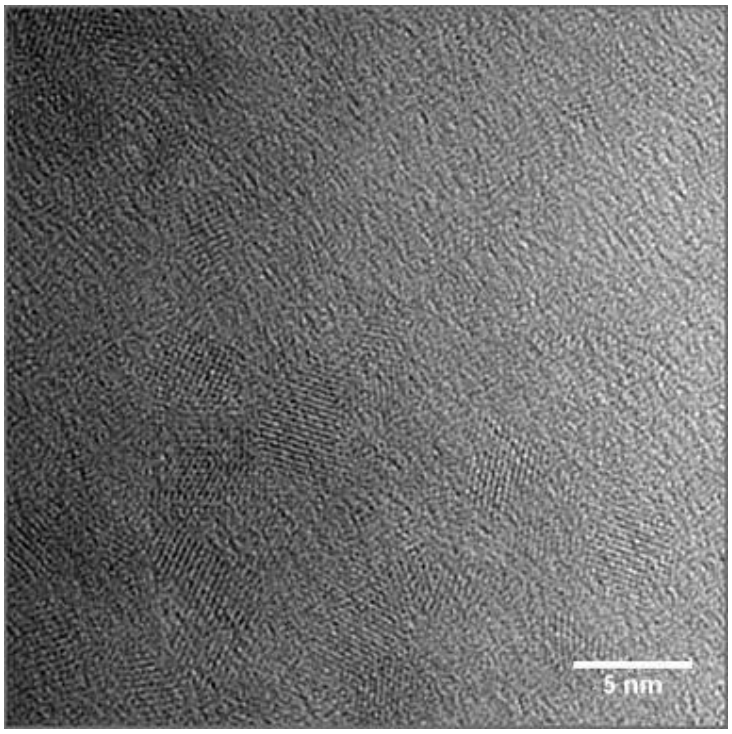

Figure 5. HRTEM image of ZnO nanoparticles. The crystalline nature of the ZnO nanoparticles is evidenced by the clearly observed lattice features.

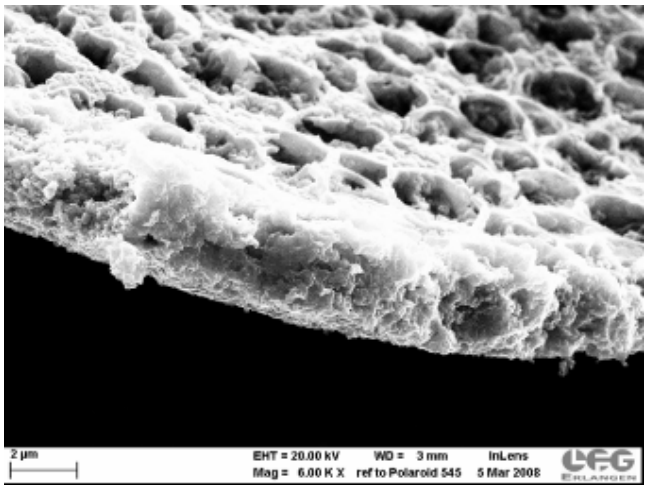

Figure 6. SEM image of a mesoporous ZnO film.

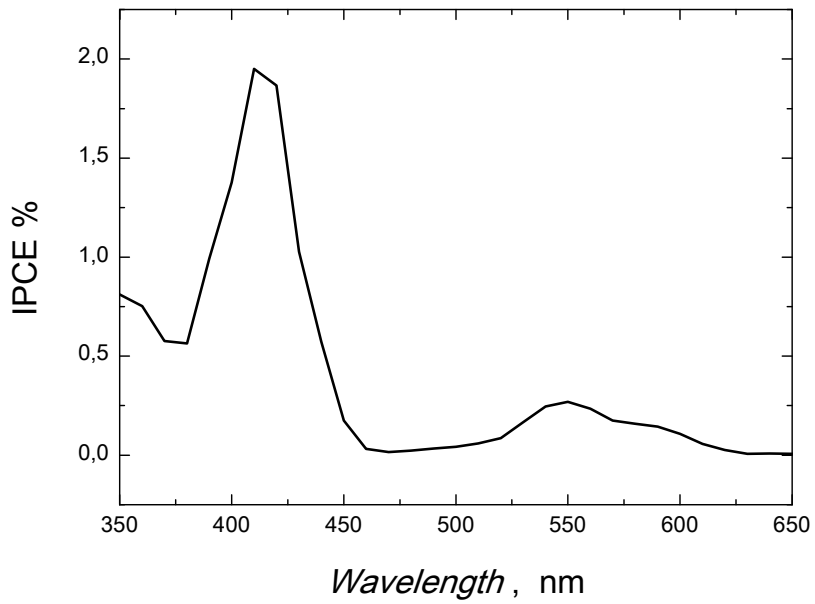

Figure 7. Photoaction spectra of the F:SnO_2/mesoporous ZnO-dye molecule/iodine-iodide/Pt cell filled with 0.6 M DMPII, 0.1 M LiI and 0.05 M Iodine in methoxyacetonitrile supporting electrolyte. Photocurrents were recorded upon monochromatic light illumination with no bias voltage being applied.